Joint Iterative Synchronization and Decoding Assisted by Pilot Symbols

Susanne Godtmann*, André Pollok*, Niels Hadaschik*, Wolfgang Steinert†, Gerd Ascheid* and Heinrich Meyr*
*Institute for Integrated Signal Processing Systems, RWTH Aachen University, Templergraben 55, 52056 Aachen, Germany
†AUDENS Telecommunications Consulting GmbH, P.O. Box 1324, 71503 Backnang, Germany

***Abstract*— In this paper we examine joint iterative synchronization and decoding in the presence of carrier frequency uncertainties and phase offsets. This approach, also referred to as turbo synchronization, exploits soft information available at the decoder output in order to support receiver synchronization. Turbo synchronization can achieve high estimation accuracy provided that the parameter offsets are sufficiently small. As this requirement is not necessarily met in realistic systems, coarse synchronization based on known pilot symbols is required for initialization. In this paper, we examined to what extent the reuse of these pilot symbols within the turbo synchronization stage can support the iterative estimation process.**

I. Introduction

With the invention of turbo codes [1], iteratively operating receivers have moved more and more into the focus of research. As compared to non-iterative receiver structures, such systems are capable of achieving a certain bit error rate (BER) at significantly reduced signal-to-noise ratios (SNR).

When considering transmission over a radio channel, offsets in timing, carrier phase and frequency may occur between transmitter and receiver due to mismatches and instabilities of the respective oscillators. Accurate frequency synchronization is of particular importance as even small mismatches severely degrade the system performance in terms of BER. However, parameter estimation in receivers utilizing iterative decoding is quite challenging as transmission occurs at low SNR [2].

Conventional synchronizers perform estimation and correction of channel parameters prior to decoding. At low SNR, these synchronizers are usually operated in the so-called data-aided (DA) mode, where the estimation process is solely based on known pilot symbols. However, as the transmission of pilot symbols reduces the spectral efficiency of the system, it is desirable to keep their number as small as possible.

The integration of synchronization into the iterative decoding process, commonly referred to as turbo synchronization [3], is a promising approach to deal with the above-mentioned challenges. The basic idea is to use the soft information which is available after each decoding step to compute so-called soft symbols. With the aid of these soft symbols, parameter estimates are generated and subsequently used to correct the received signal prior to performing further decoding iterations. As shown in various publications, e.g. [4] and [5], turbo synchronizers can achieve a performance in terms of estimation accuracy equivalent to that of DA estimation, even though only unknown data symbols are exploited. According to [3], turbo synchronization can be mathematically described by means of the Expectation Maximisation (EM) theory [6].

In order to enable convergence of the decoding process towards low BER, turbo synchronization needs to be initialized with sufficiently accurate estimates of the considered channel parameters. The range within which the residual offsets are required to lie is commonly referred to as acquisition range. As the acquisition range is quite small, especially for carrier frequency estimation, a stage for coarse synchronization is essential for the initialization of the turbo synchronizer.

An iterative coarse synchronization scheme based on both data symbols and pilot symbols has been investigated in [7]. However, note that [7] considers random data symbols and does not exploit the structure of a channel code.

The integration of pilot symbols into a code-aided iterative synchronization procedure is proposed in principle in [8] for phase offset estimation. The benefits of pilot symbols for turbo synchronization are not analyzed. The suggested approach refrains from using pilot symbols to conserve the spectral efficiency and resorts to NDA initialized hypothesis testing instead. Applying this concept does not suffice to combat frequency offsets at low SNR.

In this paper, we investigate joint iterative synchronization and decoding in the presence of frequency and phase offsets. The contribution of this work is to examine to what extent turbo synchronization can be supported by pilot symbols and how turbo synchronization performs in a realistic scenario with random parameter offsets. Furthermore, we propose a new low-complexity carrier frequency estimator suitable for turbo synchronization.

After introducing the transmission model in Section II, we present how maximum likelihood (ML) estimation can be iteratively performed through the EM algorithm. As the frequency estimator derived from EM theory is rather complex, we present a low-complexity alternative in Section IV. In order to illustrate the benefits of integrating pilot symbols into turbo synchronization, simulation results are presented in Section V.

II. Transmission Model

The transmission model considered in this paper is shown in Fig. 1. Information bits are grouped into packets, encoded and mapped onto a modulation alphabet $\mathcal{A}$. The resulting K_d data symbols are then transmitted over an additive white Gaussian noise (AWGN) channel together with K_p pilot symbols. The total number of symbols per burst is denoted as $K = K_d + K_p$.

This work has been financed by BMBF, the German Federal Ministry of Education and Research and supported by DLR, the German Aerospace Center. Special thanks go to Dr. M. Keller. S. Godtmann thanks the Deutsche Telekom Stiftung for its financial support.

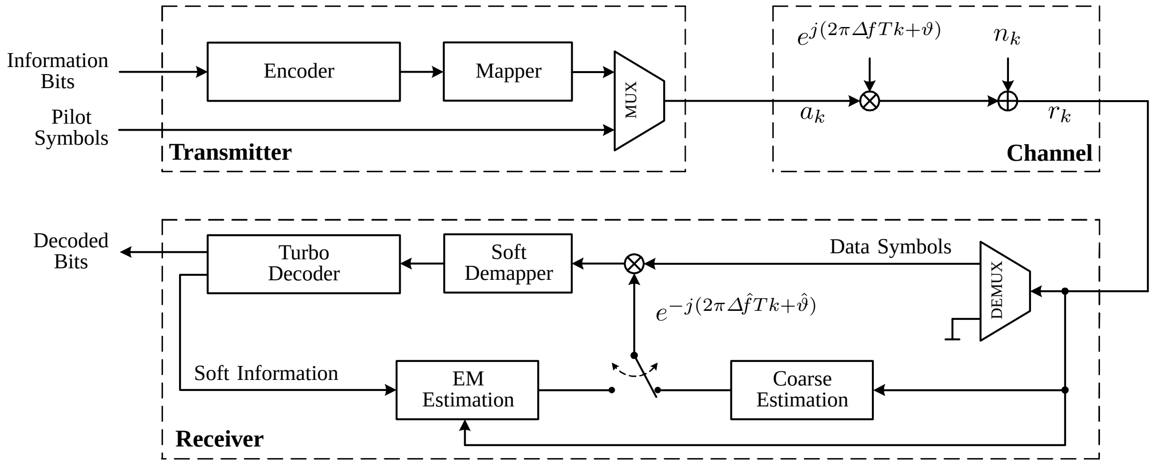

Figure 1. System Model

Under the assumption of perfect symbol timing, the received baseband signal after matched filtering and sampling can be modelled as

$$r_k = a_k \cdot e^{j(2\pi\Delta fTk+\vartheta)} + n_k, \tag{1}$$

with T being the symbol duration. The transmitted and the received symbol at sampling instant k are denoted as a_k and r_k, respectively. Unit energy symbols are assumed, i.e. $E_s = E\{|a_k|^2\} = 1$. Furthermore, n_k are the samples of complex-valued AWGN with independent real and imaginary parts, each having zero-mean and variance $N_0/(2E_s)$, where N_0 denotes the one-sided power spectral density of the noise process. In addition to the noise component, a phase offset ϑ and a frequency offset Δf are introduced by the physical channel and the oscillators. As we will focus on the transmission of short bursts, phase and frequency offset can be assumed to be constant for the duration of one burst.

Let the time scale of each burst be defined such that the innermost symbol corresponds to $k = 0$. Furthermore, let $\mathcal{K}$ denote the entire set of time instants. The subsets $\mathcal{K}_d$ and $\mathcal{K}_p$ are related to data and pilot symbols. We place one half of the pilot symbols at the beginning and the other half at the end of the burst as this setup is optimal for frequency estimation [9]. For later use, we define the K-dimensional vectors $\boldsymbol{r}$ and $\boldsymbol{a}$ as the concatenation of the symbols r_k and a_k, respectively.

III. ML Estimation through EM Algorithm

In order to illustrate the Expectation Maximisation (EM) approach, let us first consider estimation solely based on unknown data symbols [3] at the time instances in $\mathcal{K}_d$. The random vector $\boldsymbol{r}$ of channel observations depends on the vector $\boldsymbol{a}$ and on a deterministic parameter vector $\boldsymbol{b}$. As the transmitted sequence $\boldsymbol{a}$ is unknown at the receiver, it can be interpreted as a nuisance vector. The maximum likelihood (ML) estimate of $\boldsymbol{b}$ can be computed as

$$\hat{\boldsymbol{b}}_{\text{ML}} = \arg\max_{\tilde{\boldsymbol{b}}} \left\{ \ln p(\boldsymbol{r}|\tilde{\boldsymbol{b}}) \right\}, \tag{2}$$

where $\tilde{\boldsymbol{b}}$ is a trial vector of the parameter set and $p(\boldsymbol{r}|\boldsymbol{b})$ can be computed according to

$$p(\boldsymbol{r}|\boldsymbol{b}) = \int_{\boldsymbol{a}} p(\boldsymbol{r}|\boldsymbol{a},\boldsymbol{b})\; p(\boldsymbol{a})\; d\boldsymbol{a}. \tag{3}$$

In many cases, the analytical solution of (3) is intractable, making the use of iterative numerical methods inevitable.

The EM approach [6] is a method that iteratively implements ML estimation. Each iteration of the EM algorithm disintegrates into an expectation step

$$\mathcal{Q}\left(\boldsymbol{b}\middle|\hat{\boldsymbol{b}}_{\text{EM}}^{(n-1)}\right) = \int_{\boldsymbol{a}} \ln p(\boldsymbol{r}|\boldsymbol{a},\boldsymbol{b})\; p(\boldsymbol{a}|\boldsymbol{r},\hat{\boldsymbol{b}}_{\text{EM}}^{(n-1)})\; d\boldsymbol{a}, \tag{4}$$

and a maximization step

$$\hat{\boldsymbol{b}}_{\text{EM}}^{(n)} = \arg\max_{\tilde{\boldsymbol{b}}} \left\{ \mathcal{Q}\left(\tilde{\boldsymbol{b}}\middle|\hat{\boldsymbol{b}}_{\text{EM}}^{(n-1)}\right) \right\}. \tag{5}$$

The superscript (n) denotes the iteration index. The estimate $\hat{\boldsymbol{b}}_{\text{EM}}^{(n)}$ improves from iteration to iteration and converges towards the ML estimate under fairly general conditions [10].

Neglecting additive terms and a constant factor irrelevant for maximization, the log-likelihood function $\ln p(\boldsymbol{r}|\boldsymbol{a},\boldsymbol{b})$ for the considered transmission model can be expressed as

$$\ln p(\boldsymbol{r}|\boldsymbol{a},\boldsymbol{b}) = \text{Re}\left\{ \sum_{k\in\mathcal{K}_d} r_k\; a_k^*\; e^{-j(2\pi\Delta fTk+\vartheta)} \right\}, \tag{6}$$

with the parameter vector $\boldsymbol{b} = [\vartheta, \Delta f]^{\text{T}}$.

Let us – in accordance with [3] – define a-posteriori average values of the transmitted symbols a_k as

$$\begin{aligned}\alpha_k\left(\boldsymbol{r},\hat{\boldsymbol{b}}_{\text{EM}}^{(n-1)}\right) &= \int_{\boldsymbol{a}} a_k^*\; p\left(\boldsymbol{a}\middle|\boldsymbol{r},\hat{\boldsymbol{b}}_{\text{EM}}^{(n-1)}\right)\; d\boldsymbol{a} \\ &= \sum_{a\in\mathcal{A}} a\; P\left(a_k = a\middle|\boldsymbol{r},\hat{\boldsymbol{b}}_{\text{EM}}^{(n-1)}\right).\end{aligned} \tag{7}$$

Substituting (6) into (4), we finally obtain

$$\begin{aligned}&\mathcal{Q}\left(\boldsymbol{b}\middle|\hat{\boldsymbol{b}}_{\text{EM}}^{(n-1)}\right) \\ &\quad= \text{Re}\left\{ \sum_{k\in\mathcal{K}_d} r_k\; e^{-j(2\pi\Delta fTk+\vartheta)}\; \alpha_k^*\left(\boldsymbol{r},\hat{\boldsymbol{b}}_{\text{EM}}^{(n-1)}\right) \right\}.\end{aligned} \tag{8}$$

Maximization of the latter expression, i.e. carrying out the maximization step (5), yields the EM estimators:

$$\Delta\hat{f}_{\text{EM}}^{(n)} = \arg\max_{\Delta\tilde{f}} \left\{ \left| \sum_{k\in\mathcal{K}_d} r_k\; e^{-j2\pi\Delta\tilde{f}Tk} \alpha_k^*\left(\boldsymbol{r},\hat{\boldsymbol{b}}_{\text{EM}}^{(n-1)}\right) \right| \right\} \tag{9}$$

$$\hat{\vartheta}_{\text{EM}}^{(n)} = \arg\left\{ \sum_{k\in\mathcal{K}_d} r_k\; e^{-j2\pi\Delta\hat{f}_{\text{EM}}^{(n)}Tk} \alpha_k^*\left(\boldsymbol{r},\hat{\boldsymbol{b}}_{\text{EM}}^{(n-1)}\right) \right\}. \tag{10}$$

Note that a phase estimate can be obtained analytically, while an expensive maximum search emerges from the EM rule for frequency estimation.

A. Soft–Decision–Directed Turbo Synchronization

As can be seen from (7), the symbols α_k depend on a-posteriori probabilities $P\big(a_k = a|\boldsymbol{r}, \hat{\boldsymbol{b}}_{\mathrm{EM}}^{(n-1)}\big)$. The soft information provided by a turbo decoder can be used for their approximation. This immediately suggests to perform synchronization and iterative soft decoding jointly. In order to obtain reliable soft information, decoding needs to be performed until its convergence. However, this results in unacceptably high computational complexity. Therefore, as proposed in [3], we carry out only one single decoding step prior to update the estimates. As the entire set of α_k is required, the turbo decoder needs to be slightly modified in order to generate soft information for all encoded bits and not only for the information bits.

After coarse synchronization is completed, the switch in Fig. 1 is toggled to its left position, closing the turbo synchronization loop. As soon as one decoding iteration is completed, the available soft information is passed on to the EM estimation unit. Based on the refined parameter estimates, the received sequence of data symbols is corrected prior to performing further decoding steps. As synchronization and decoding are performed jointly, both estimates and decoding results progressively benefit from mutual improvements. In the case of convergence, the soft symbols α_k can be considered equivalent to the transmitted symbols a_k. According to [4], this approach is referred to as soft-decision-directed (SDD) turbo synchronization.

B. SDD Turbo Synchronization Assisted by Pilot Symbols

In the case that pilot symbols are available at the receiver, the summation in (8) over the subset $\mathcal{K}_d$ needs to be replaced by a summation over all time instants in the set $\mathcal{K}$ [8]. Taking into account that for $k \in \mathcal{K}_p$ the soft symbols α_k can be substituted by known pilot symbols a_k, we find

$$\mathcal{Q}'\Big(\boldsymbol{b}|\hat{\boldsymbol{b}}_{\mathrm{EM}}^{(n-1)}\Big) = \mathrm{Re}\Bigg\{\sum_{k\in\mathcal{K}_d} r_k\, e^{-j(2\pi\Delta f T k+\vartheta)}\alpha_k^*\Big(\boldsymbol{r}, \hat{\boldsymbol{b}}_{\mathrm{EM}}^{(n-1)}\Big)\Bigg\} + \underbrace{\mathrm{Re}\Bigg\{\sum_{k\in\mathcal{K}_p} r_k\, e^{-j(2\pi\Delta f T k+\vartheta)}a_k^*\Bigg\}}_{=\mathcal{Q}^{\mathrm{DA}}}. \quad (11)$$

Obviously, the accuracy of the estimates can be improved when the estimation process is based on K instead of K_d symbols. As will be demonstrated in Section V, the use of known symbols is also beneficial for the convergence properties of the iterative synchronization procedure. Especially during the first EM iterations, estimation purely based on soft symbols is often corrupted by unreliable soft information [3]. Then, the contribution of $\mathcal{Q}^{\mathrm{DA}}$ in (11) helps to adjust the estimates towards the true values of the parameter offsets.

IV. Generalized SDD Estimation

Since the EM rule for frequency estimation (9) requires a computationally expensive maximum search, it is desirable to find an estimator with reduced complexity. In the previous section, it was indicated that, in the case of convergence, the soft symbols α_k tend towards the transmitted symbols a_k. As the demodulated received symbols $z_k = r_k a_k^*$ can therefore be approximated by $z_k = r_k \alpha_k^*$, conventional data-aided estimators can also be operated in SDD mode.

In this section, frequency estimation by means of linear regression [11] is considered. Due to the assumption that both carrier phase and frequency offset remain constant for the duration of one burst, the vector $\boldsymbol{z} = [z_1, \ldots, z_K]^{\mathrm{T}}$ is characterized by a linear phase, only disturbed by AWGN. The basic idea is now to determine constant offset and slope of this linear function from the set $\boldsymbol{z}$ of noisy samples. Regression analysis, based on the minimum mean square error criterion, offers a technique to estimate both parameters. In our case, a regression of first order is required, meaning that the regression line between all phase angles $\varphi_k = \arg\{z_k\}$ needs to be determined. According to [11], an estimate of the frequency offset can be computed as

$$\Delta\hat{f} = \frac{1}{2\pi T}\,\frac{\sum_{k\in\mathcal{K}}\left(k-\bar{k}\right)\left(\varphi_k-\bar{\varphi}\right)}{\sum_{k\in\mathcal{K}}\left(k-\bar{k}\right)^2}, \quad (12)$$

where $\bar{k}$ and $\bar{\varphi}$ denote the mean of time index and phase angle, respectively. The estimate of the constant phase ϑ can subsequently be obtained from

$$\hat{\vartheta} = \bar{\varphi} - 2\pi\Delta\hat{f}T\bar{k}. \quad (13)$$

In practical cases, the linear phase might be severely corrupted due to rather low SNR. In order to obtain more precise estimates, a modified approach averages over a certain number of unmodulated symbols prior to determining their phase angles. To do so, the burst is subdivided into M blocks and the K_m symbols within each block are subsequently summed up. Due to the summation, the averaged symbols are characterized by an increased SNR. Let $\bar{k}_m$ denote the position of the average symbol of the m^{th} block and let $\bar{\varphi}_m$ denote its phase. Then, the estimator for the carrier frequency can finally be expressed as

$$\Delta\hat{f} = \frac{1}{2\pi T}\,\frac{\sum_{m=1}^{M}\left(\bar{k}_m-\bar{k}\right)\left(\bar{\varphi}_m-\bar{\varphi}\right)}{\sum_{m=1}^{M}\left(\bar{k}_m-\bar{k}\right)^2}, \quad (14)$$

and the phase estimate can be directly obtained by inserting (14) into (13).

Assuming that M is sufficiently large, it can be demonstrated by means of simulations that the EM estimator (9) and the linear regression estimator (14) show virtually the same performance in terms of estimation accuracy.

V. Simulations

All simulations presented in this paper are based on DVB-RCS[1] [12]. With DVB-RCS, a standard has been introduced whose implementation is very challenging due to transmission at low SNR coupled with short burst lengths. As turbo encoding is used as one possible encoding scheme in DVB-RCS, this standard is suitable to analyze the performance of turbo synchronization.

[1] Digital Video Broadcasting – Return Channel via Satellite

For our investigations, we consider bursts with 16 bytes. This burst format is used in DVB-RCS for signalling and synchronization purposes. The code rate is chosen as $r=1/3$ and QPSK modulation is used. This results in $K_d = 192$ transmitted symbols. The ratio of energy per information bit and N_0 is fixed at $E_b/N_0=2\,\text{dB}$.

As DVB-RCS is supposed to operate with low cost transmitters, instabilities of the oscillators can lead to frequency offsets of more than one order of magnitude higher than those turbo synchronization can cope with. Thus, the use of a coarse synchronization unit relying on pilot symbols is essential. Since the block length is fixed due to the standard, data symbols cannot be replaced by pilot symbols, but pilot symbols need to be provided additionally. We define the ratio of the number of pilot symbols and the total number of symbols per burst as $\eta = K_p/(K_d + K_p)$. The DVB-RCS standard does not specify a certain overhead of pilot symbols. In order to assure that the coarse synchronization unit is capable of reducing the initial parameter offsets such that the residual offsets are within the acquisition range of the turbo synchronizer, we choose $\eta = 0.2$. This can be considered adequate for such short bursts.

A. *Performance Results*

For the analysis of the estimation performance, we resort to the BER and the mean square estimation error (MSEE). In the case of an unbiased estimate $\hat{b}_i$, the MSEE is lower bounded by the Cramér-Rao bound (CRB), i.e.

$$\varepsilon_{\text{MSE}}\left\{\hat{b}_i\right\} \geq CRB_i. \qquad (15)$$

Under the assumption that the entire transmitted sequence is known at receiver side (DA case), the CRBs coincide with the so-called modified CRBs given in [13].

All results presented in this section were obtained by computer simulations based on iterative synchronization of both phase and frequency. As the complexity of the linear regression estimator (see (13) and (14)) is significantly lower than that of the EM estimator (see (9) and (10)), it was applied in all simulations presented in this paper. The parameter M was chosen to 10.

Fig. 2 depicts the MSEE versus a normalized fixed residual frequency offset $\varepsilon_{\Delta f}=\Delta f-\Delta\hat{f}^{(0)}_{\text{EM}}$. If coarse synchronization has been carried out, $\Delta\hat{f}^{(0)}_{\text{EM}}$ would be the estimate generated by the coarse synchronization unit. The residual phase offset $\varepsilon_\vartheta=\vartheta-\vartheta^{(0)}_{\text{EM}}$ is set to zero. However, since perfect estimation is impossible, the instantaneous phase offset will not remain zero throughout the iterative estimation process. The graphs from top to bottom correspond to the situation after completion of one, three, and ten iterations. Circular markers correspond to purely SDD turbo synchronization (see Section III-A), cross markers to SDD-DA turbo synchronization (see Section III-B). The lower bounds for purely SDD estimation and the SDD-DA approach are denoted as $CRB^{\text{DA}}_{\Delta f}(K_d)$ and $CRB^{\text{DA}}_{\Delta f}(K_d{+}K_p)$, respectively. After convergence, both algorithms perform very closely to their optimum within their acquisition range. However, the acquisition range of pilot-assisted synchronization is about twice as large as that of purely SDD synchronization. Due to the increased number of channel observations, the estimation accuracy is also slightly improved when pilot symbols are integrated into the iterative synchronization process.

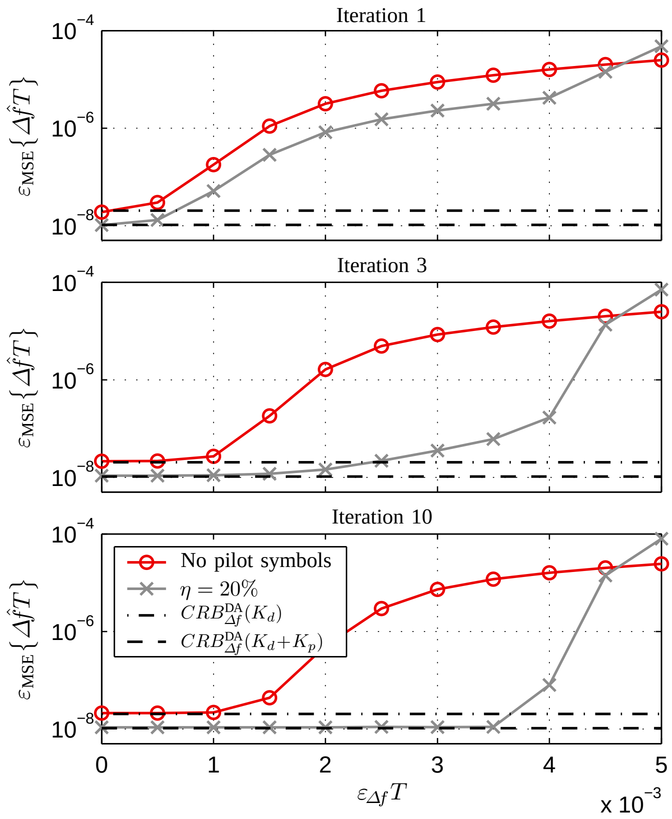

Figure 2. MSEE vs. Frequency Offset; Phase Offset $\varepsilon_\vartheta = 0$

As yet, it has been investigated how turbo synchronization performs in the presence of small parameter offsets with a fixed magnitude. As it is the task of the turbo synchronization stage to refine the estimates $\hat{b}^{(0)}_i$ provided by a stage for coarse synchronization, it needs to combat random offsets in realistic scenarios. Their variance $\sigma^2_{b_i}$ is required to be so small that the acquisition range of the turbo synchronizer, limited by $\pm\varepsilon_{b_i,\max}$, is exceeded only with a certain probability P.

The limits $\varepsilon_{b_i,\max}$ of the acquisition range depend on the block length, the SNR, the channel code and the code rate. For our simulation scenario, purely SDD turbo synchronization yields $\varepsilon_{\vartheta,\max} = 28°$ and $\varepsilon_{\Delta f,\max}T = 1.2\cdot10^{-3}$. These values were obtained by means of simulation and $\varepsilon_{\Delta f,\max}T$ may also be inferred from Fig. 2.

In realistic systems, P depends on the algorithm used for coarse synchronization and on the overhead of pilot symbols within a burst. However, as we want to abstract from coarse synchronization, we choose a fixed probability P.

The convergence speed of the decoding process for SDD turbo synchronization and SDD-DA synchronization is illustrated in Fig. 3(a) and Fig. 3(b), respectively. The residual offsets of frequency and phase are normally distributed having zero mean. Their variances are chosen such that the acquisition range of SDD turbo synchronization is exceeded with $P=P\left\{|\varepsilon_{b_i}| > \varepsilon_{b_i,\max}\right\}$. The dashed lines with circular markers show the BER performance without any synchronization and are therefore identical in both figures. Keeping in mind that the objective is to ensure a certain BER, it becomes ap-

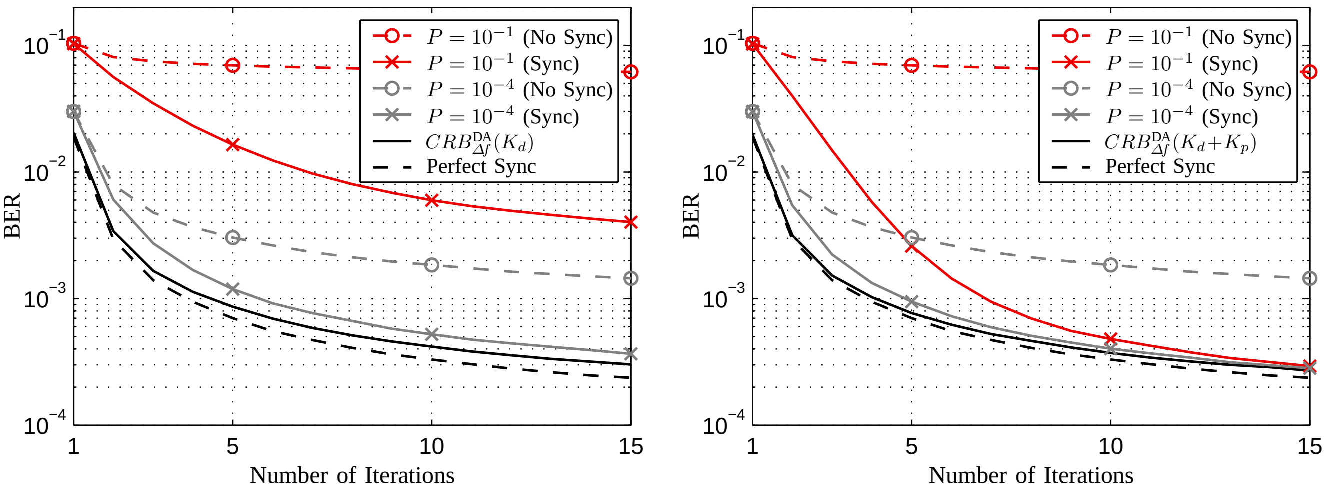

(a) SDD Synchronization

(b) SDD-DA Synchronization

Figure 3. BER vs. Iterations; $\varepsilon_\vartheta \sim \mathcal{N}(0,\sigma_\vartheta^2)$, $\varepsilon_{\Delta f} \sim \mathcal{N}(0,\sigma_{\Delta f}^2)$

parent that joint synchronization and decoding (cross markers) attains this BER after fewer iterations. As synchronization is significantly less complex than turbo decoding, the complexity of the whole system can be reduced by employing turbo synchronization. In both figures, the undermost line corresponds to the ideal case without synchronization errors. The solid curve just above shows the decoding behavior when optimal synchronization is carried out. It was obtained by restricting the simulation to decoding in the presence of normally distributed residual offsets with variances $\sigma_{b_i}^2 = CRB^{\mathrm{DA}}(K_d)$ and $CRB^{\mathrm{DA}}(K_d+K_p)$, respectively. Thus, for assessing the convergence speed of our system, this curve represents the benchmark. In Fig. 3(a), it becomes apparent that large initial parameter offsets cause severe degradations of the decoding performance. The convergence speed during the first iterations is slowed down and the asymptotic performance is reduced dramatically. Regarding Fig. 3(b) in comparison to Fig. 3(a), it can be seen that both convergence speed and asymptotic behavior are improved considerably by SDD-DA turbo synchronization. As already mentioned, speeding up the decoding process can significantly reduce the overall computational complexity. It should be stressed that both simulations were run with the same distribution of residual phase and frequency offsets at the same SNR.

VI. Conclusion

In this paper, we perform carrier synchronization and decoding jointly by applying the principle of turbo synchronization. In contrast to the standard approach [3], which exclusively exploits unknown data symbols, we illustrate the benefits of integrating known pilot symbols into the iterative estimation procedure. Pilot-assisted turbo synchronization can cope with larger initial parameter offsets and exhibits significantly improved performance, in both estimation accuracy and speed of convergence. Furthermore, we demonstrate that the theoretically optimal frequency estimator can be replaced by a solution of considerably reduced computational complexity.

References

[1] C. Berrou, A. Glavieux, P. Thitimajshima, "Near Shannon Limit Error-Correcting Coding and Decoding: Turbo-Codes (1)," in *Proc. of IEEE International Conference on Communications (ICC)*, vol. 2, Geneva, Switzerland, May 1993, pp. 1064–1070.

[2] H. Meyr, M. Moeneclaey, S. Fechtel, *Digital Communication Receivers: Synchronization, Channel Estimation and Signal Processing*, 1st ed. New York, NY: John Wiley & Sons, 1998.

[3] N. Noels, C. Herzet, A. Dejonghe, V. Lottici, H. Steendam, M. Moeneclaey, M. Luise, L. Vandendorpe, "Turbo Synchronization: An EM Algorithm Interpretation," in *Proc. of IEEE International Conference on Communications (ICC)*, vol. 4, Anchorage, Alaska, USA, May 2003, pp. 2933–2937.

[4] V. Lottici, M. Luise, "Embedding Carrier Phase Recovery Into Iterative Decoding of Turbo-Coded Linear Modulations," *IEEE Transactions on Communications*, vol. 52, no. 4, pp. 661–669, Apr. 2004.

[5] L. Zhang, A. G. Burr , "Iterative Carrier Phase Recovery Suited to Turbo-Coded Systems," *IEEE Transactions on Wireless Communications*, vol. 3, no. 6, pp. 2267–2276, Nov. 2004.

[6] A. P. Dempster, N. M. Laird, D.B. Rubin, "Maximum-Likelihood from Incomplete Data via the EM Algorithm," *Journal of the Royal Statistical Society, Series B*, vol. 39, no. 1, pp. 1–38, Jan. 1977.

[7] N. Noels, H. Steendam, M. Moeneclaey, "Pilot-Symbol Assisted Iterative Carrier Synchronization for Burst Transmission," in *Proc. of IEEE International Conference on Communications (ICC)*, vol. 1, Paris, France, June 2004, pp. 509–513.

[8] H. Wymeersch, M. Moeneclaey, "Iterative Code-Aided ML Phase Estimation and Phase Ambiguity Resolution," *Eurasip Journal on Applied Signal Processing. Special Issue on Turbo Processing*, vol. 2005, no. 6, pp. 981–988, May 2005.

[9] J.A. Gansman, J.V. Krogmeier, M.P. Fitz, "Single Frequency Estimation with Non-Uniform Sampling," in *Proc. of 30th Asilomar Conference on Signals, Systems and Computers*, vol. 1, Pacific Grove, California, USA, Nov. 1996, pp. 399–403.

[10] C. F. J. Wu, "On the Convergence Properties of the EM Algorithm," *The Annals of Statistics*, vol. 11, no. 1, pp. 95–103, 1983.

[11] S. A. Tretter, "Estimating the Frequency of a Noisy Sinusoid by Linear Regression," *IEEE Transactions on Information Theory*, vol. 31, no. 6, pp. 832–835, Nov. 1985.

[12] ETSI, "Digital Video Broadcasting (DVB); Interaction Channel for Satellite Distribution Systems (EN 301 790 V1.4.1)," Apr. 2005.

[13] A. N. D'Andrea, U. Mengali, R. Reggiannini, "The Modified Cramér-Rao Bound and Its Application to Synchronization Problems," *IEEE Transactions on Communications*, vol. 42, no. 2/3/4, pp. 1391–1399, Feb.-Apr. 1994.